Submitted to ApJ 2008-11-07, accepted 2009-02-11.
Preprint typeset using LaTeX style emulateapj v. 03/07/07

arXiv:0811.1044v2 [astro-ph] 27 Feb 2009

GRB 080503: IMPLICATIONS OF A NAKED SHORT GAMMA-RAY BURST DOMINATED BY EXTENDED EMISSION

D. A. Perley[1], B. D. Metzger[1], J. Granot[2], N. R. Butler[1], T. Sakamoto[3,4], E. Ramirez-Ruiz[5], A. J. Levan[6], J. S. Bloom[1,7], A. A. Miller[1], A. Bunker[8,9], H.-W. Chen[10], A. V. Filippenko[1], N. Gehrels[3], K. Glazebrook[11], P. B. Hall[12], K. C. Hurley[13], D. Kocevski[14], W. Li[1], S. Lopez[15], J. Norris[16], A. L. Piro[1], D. Poznanski[1], J. X. Prochaska[5], E. Quataert[1], N. Tanvir[17]

Submitted to ApJ 2008-11-07, accepted 2009-02-11.

ABSTRACT

We report on observations of GRB 080503, a short gamma-ray burst with very bright extended emission (about 30 times the gamma-ray fluence of the initial spike) in conjunction with a thorough comparison to other short *Swift* events. In spite of the prompt-emission brightness, however, the optical counterpart is extraordinarily faint, never exceeding 25 mag in deep observations starting at ∼1 hr after the BAT trigger. The optical brightness peaks at ∼ 1 day and then falls sharply in a manner similar to the predictions of Li & Paczyński (1998) for supernova-like emission following compact-binary mergers. However, a shallow spectral index and similar evolution in X-rays inferred from *Chandra* observations are more consistent with an afterglow interpretation. The extreme faintness of this probable afterglow relative to the bright gamma-ray emission argues for a very low-density medium surrounding the burst (a "naked" GRB), consistent with the lack of a coincident host galaxy down to 28.5 mag in deep *Hubble Space Telescope* imaging. The late optical and X-ray peak could be explained by a slightly off-axis jet or by a refreshed shock. Our observations reinforce the notion that short gamma-ray bursts generally occur outside regions of active star formation, but demonstrate that in some cases the luminosity of the extended prompt emission can greatly exceed that of the short spike, which may constrain theoretical interpretation of this class of events. This extended emission is not the onset of an afterglow, and its relative brightness is probably either a viewing-angle effect or intrinsic to the central engine itself. Because most previous BAT short bursts without observed extended emission are too faint for this signature to have been detectable even if it were present at typical level, conclusions based solely on the observed presence or absence of extended emission in the existing *Swift* sample are premature.

Subject headings: gamma rays: bursts — gamma-ray bursts: individual: 080503

1. INTRODUCTION

Despite significant progress since the launch of the *Swift* satellite (Gehrels et al. 2004), the origin of short-duration, hard-spectrum gamma-ray bursts (SGRBs) remains elusive. Evidence has been available since the early 1990s that SGRBs constitute a separate class from longer GRBs on the basis of a bimodal distribution in duration (Mazets et al. 1981; Norris et al. 1984) and spectral hardness (Kouveliotou et al. 1993). The supposition that this phenomenological divide is symptomatic of a true physical difference in the origin of the events was supported by the first successful localizations of SGRB afterglows with the *Swift* X-ray telescope (Burrows et al. 2005) coincident with or apparently very near low-redshift ($z < 0.5$) galaxies (Gehrels et al. 2005; Fox et al. 2005). Several of these galaxies clearly lack significant recent star formation (e.g., Prochaska et al. 2006; Gorosabel et al. 2006; Berger et al. 2005), many events appeared at large offset from the candidate host (Bloom et al. 2006, 2007; Stratta et al. 2007), and in some cases the appearance of a bright supernova was definitively ruled out (e.g., Hjorth et al. 2005a). All of these circumstantial clues seem to suggest (Lee & Ramirez-Ruiz 2007; Nakar 2007) a progenitor very different from the one responsible for long-duration GRBs (LGRBs), which are predominately due to the deaths of massive stars (see Woosley & Bloom 2006 for a review).

The generally favored interpretation of SGRBs is

[1] Department of Astronomy, University of California, Berkeley, CA 94720-3411.
[2] Centre for Astrophysics Research, University of Hertfordshire, College Lane, Hatfield, Herts, AL10 9AB, UK.
[3] NASA Goddard Space Flight Center, Greenbelt, MD 20771.
[4] CRESST/Joint Center for Astrophysics, University of Maryland, Baltimore County, Baltimore, MD 21250.
[5] Department of Astronomy and Astrophysics, UCO/Lick Observatory, University of California, 1156 High Street, Santa Cruz, CA 95064.
[6] Department of Physics, University of Warwick, Coventry CV4 7AL, UK.
[7] Sloan Research Fellow.
[8] School of Physics, University of Exeter, UK
[9] Anglo-Australian Observatory
[10] Department of Astronomy and Astrophysics, University of Chicago, 5640 S. Ellis Ave, Chicago, IL 60637.
[11] Swinburne University of Technology
[12] Department of Physics and Astronomy, York University, 4700 Keele St., Toronto, Ontario M3J 1P3, Canada
[13] University of California, Berkeley, Space Sciences Laboratory, 7 Gauss Way, Berkeley, CA 94720-7450
[14] Kavli Institute for Particle Astrophysics and Cosmology, Stanford University, 2575 Sand Hill Road M/S 29, Menlo Park, CA 94025
[15] Departamento de Astronomía, Universidad de Chile, Casilla 36-D, Santiago, Chile
[16] University of Denver, Physics and Astronomy Department, Denver, CO 80208
[17] Department of Physics and Astronomy, University of Leicester, University Road, Leicester LE1 7RH

the merger of two highly compact degenerate objects: two neutron stars (NS–NS, Eichler et al. 1989; Meszaros & Rees 1992; Narayan et al. 1992) or a neutron star and a black hole (NS–BH, Paczynski 1991; Narayan et al. 1992; Mochkovitch et al. 1993; Kluzniak & Lee 1998; Janka et al. 1999). However, other progenitor models (e.g., MacFadyen et al. 2005; Metzger et al. 2008a) can also be associated with galaxies having low star-formation rates (SFRs), and many SGRBs have also been associated with relatively low-luminosity, high-SFR galaxies (Fox et al. 2005; Hjorth et al. 2005b; Covino et al. 2006; Levan et al. 2006) and at much higher redshifts (Berger et al. 2007; Cenko et al. 2008) than the better-known elliptical hosts of the first few well-localized SGRBs 050509B and 050724. (A review of SGRB progenitor models is given by Lee & Ramirez-Ruiz 2007.)

In addition, even the conventional distinction between SGRBs and LGRBs has been called into question by some recent events which poorly conform to the traditional classification scheme. A large number of *Swift* events which initially appeared to be "short" (based only on the analysis of the first, most intense pulse) were then followed by an additional episode of long-lasting emission with a duration of up to 100 s or longer. GRB 050724, which unambiguously occurred in an elliptical host, is a member of this class, creating a breakdown in the use of duration (in particular T_{90}, Kouveliotou et al. 1993) as a classification criterion. To further complicate the picture, long GRB 060614 exploded in a very low-SFR dwarf galaxy at $z = 0.125$ and despite an intensive follow-up campaign showed no evidence for a supernova, even if extremely underluminous ($M_V > -12.3$, Gal-Yam et al. 2006). Similar confusion clouds the physical origin of GRB 060505, which is of long duration ($T_{90} = 4 \pm 1$ s) and occurred in a star-forming region of a spiral galaxy (Thöne et al. 2008), but also lacked supernova emission to very deep limits (Fynbo et al. 2006). Two earlier bursts, XRF 040701 (Soderberg et al. 2005) and GRB 051109B (Perley et al. 2006), may constitute additional examples of this subclass, though available limits in each case are much shallower and the alternate possibility of host-galaxy extinction is poorly constrained compared to the 2006 events. On the basis of these results and others, Zhang et al. (2007) have called for a new terminology for classification that does not refer to "short" and "long" but rather to Type I and Type II GRBs, in recognition of the fact that duration alone is likely to be an imperfect proxy for physical origin (see also Gehrels et al. 2006, Bloom et al. 2008, Kann et al. 2008).

The true "smoking gun" for the merger model, the detection of gravitational waves, is unlikely to occur before the completion of the next generation of gravity-wave detectors, as the sensitivity of current detectors (LIGO, Abbott 2004; and Virgo, Acernese 2004) is several orders of magnitude below what would be necessary to detect a merger at what appears to be a "typical" short GRB redshift of 0.2–1.0 (Abbott 2008). However, degenerate-merger models do offer additional observationally verifiable predictions.

First, merger progenitors are much older than massive stars and can travel far from their birthsites, especially if they are subject to kicks which in some cases could eject the binary system progenitor from the host galaxy entirely (Fryer et al. 1999; Bloom et al. 1999). Observationally, this should manifest itself in the form of large angular offsets between the burst position and the host galaxy or even the lack of any observable host at all. Such an trend has indeed been noted for many events (e.g., Prochaska et al. 2006). The second prediction, however, has yet to be demonstrated: if some SGRBs explode in galactic halos, then the extremely low associated interstellar density will result in a much fainter afterglow associated with the external shock: a "naked" gamma-ray burst. And while the afterglows of SGRBs tend to be fainter in an absolute sense (Kann et al. 2008), relative to the gamma-ray emission (on average, SGRBs have much lower total fluences than long LGRBs) there appears to be no obvious difference between SGRB and LGRB afterglows (Nysewander et al. 2008). Part of this may be a selection effect, but the brightest SGRBs to date have all been associated with bright afterglows and cannot be "naked".

Second, during the merger process, a significant amount of neutron-rich ejecta (including $\sim 10^{-3}\mathrm{M}_{\odot}$ of radioactive Ni, Metzger et al. 2008a) is believed to be ejected at nonrelativistic velocities into interstellar space. Nucleosynthesis in this matter and the resulting radioactive decay would be expected to produce a relatively long-lived optical counterpart, similar to ordinary supernovae (Li & Paczyński 1998). Unfortunately, the luminosity of the transient is generally much lower and the timescale of evolution is significantly faster than in a classical supernova. Detection of this signature remains one of the holy grails in the study of GRBs, though deep early limits for some SGRBs have allowed some limits to be set on the physical parameters of this phenomenon (Bloom et al. 2006; Hjorth et al. 2005a; Kann et al. 2008).

In this paper, we present results from our follow-up campaign of GRB 080503, which we argue in §2.1 is a prominent example of the emerging subclass of SGRBs with extended episodes of bright, long-lasting prompt emission following the initial short spike. In §2.2–§2.7 we present additional space-based and ground-based observations of the event highlighting several extreme and unusual features of this burst, including extreme optical faintness, a late light-curve peak, and a very deep late-time limit on any coincident host galaxy. In §3 we attempt to interpret the observed behavior in the context of existing models of emission from GRB internal shocks, an unusual afterglow, and from mini-SN light, arguing that the latter is probably not a large contributor at any epoch. Finally, in §4 we discuss the implications of this event for GRB classification, and on the difficulties faced by future searches for mini-SN light associated with SGRBs.

2. OBSERVATIONS

2.1. *BAT Analysis and High-Energy Classification*

The *Swift* Burst Alert Telescope (BAT) detected GRB 080503 at 12:26:13 on 2008 May 3 (UT dates and times are used throughout this paper). The GRB light curve (Figure 1) is a classic example of a short GRB with extended emission: a short, intense initial spike with a duration of less than 1 s followed by a long episode of extended emission starting at ∼10 s and lasting for several

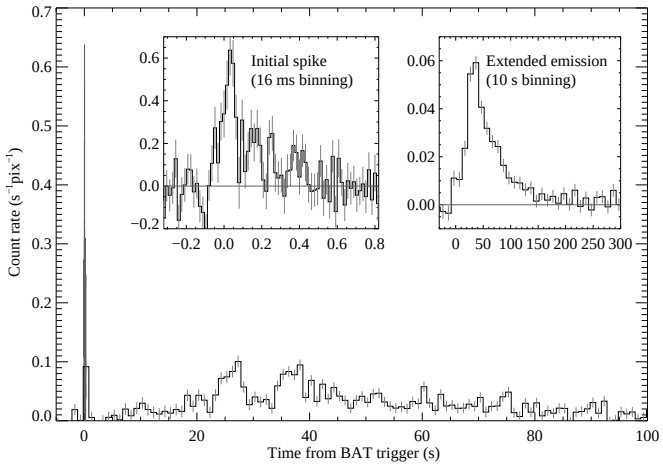

FIG. 1.— The BAT light curve of GRB 080503 with 1 s binning in the 15–150 keV band, with a 16 ms binning curve superposed for the duration of the short spike near $t = 0$. The short spike is also shown alone in the left inset. An extended, highly-binned (10 s) light curve is shown in the right inset, demonstrating the faint emission continuing until about 200 s.

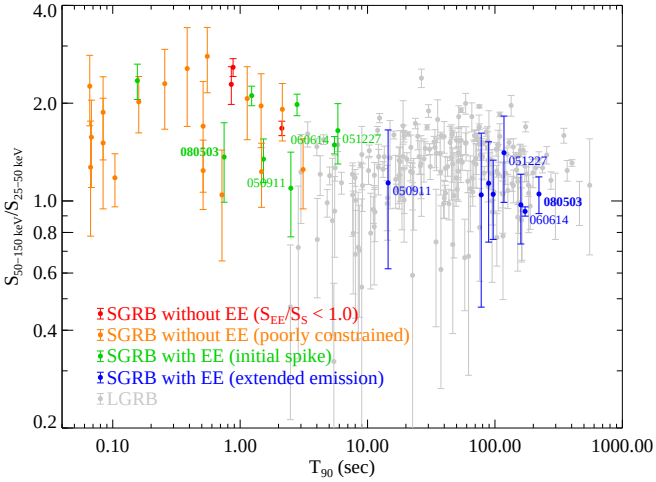

FIG. 2.— Duration-hardness plot for bursts detected by the *Swift* BAT. Long bursts are shown in gray. Short bursts ($T_{90} < 2$ sec) are colored based on the presence or absence of extended emission: bursts without extended emission are shown in red, faint bursts for which the presence of extended emission is poorly constrained are orange, and short bursts with observed extended-emission (including GRBs 050911, 060614, and 051227, whose classifications are controversial) are plotted with the short spike (green) shown separately from the extended emission (blue). The T_{90}s and hardness ratios measured for short-hard spikes in this population, including GRB 080503, are generally consistent with those measured for short bursts without extended emission. GRBs 060614 and 051227 may be consistent with both classes, but are unusually long compared to any short burst without extended emission. The extended-emission components of all three events display similar hardness and duration as the extended components of more traditional extended-emission events, which form a tight cluster (GRB 050911 is an outlier). In general, however, the hardness in the *Swift* channels is not a strong criterion for classification (Sakamoto et al. 2006; Ohno et al. 2008).

minutes. The overall T_{90} for the entire event is 232 s.

Similar extended emission has been seen before in many short bursts detected by both *Swift* and BATSE (Figure 3). All such events to date have remarkably similar general morphologies. However, the fact that the long component is so dominant in this case (factor of ∼30 in total fluence) raises the question of whether this is truly a "short" (or Type I) GRB and not an event more akin to the traditional LGRBs (Type II) in disguise. To this end we have reanalyzed the BAT data in detail and applied additional diagnostics to further investigate the nature of this event. We also downloaded and re-analyzed BAT data from all other SGRBs (and candidate SGRBs) with and without extended emission through the end of 2007. A summary of the results of our analysis is presented in Table 1.

The BAT data analysis was performed using the *Swift* HEAsoft 6.5 software package. The burst pipeline script, `batgrbproduct`, was used to process the BAT event data. In addition to the script, we made separate spectra for the initial peak and the extended emission interval by `batbinevt`, applying `batphasyserr` to the PHA files. Since the spectral interval of the extended emission includes the spacecraft slew period, we created the energy response files for every 5 s period during the time interval, and then weighted these energy response files by the 5 s count rates to create the averaged energy response. The averaged energy response file was used for the spectral analysis of the extended emission interval. Similar methods were employed for previous *Swift* SGRBs.

For GRB 080503, the T_{90} durations of the initial short spike and the total emission in the 15–150 keV band are 0.32 ± 0.07 s, and 232 s respectively. The peak flux of the initial spike measured in a 484 ms time window is $(1.2 \pm 0.2) \times 10^{-7}$ erg cm^{-2} s^{-1}. The hardness ratio between the 50–100 keV and the 25–50 keV bands for this initial spike is 1.2 ± 0.3, which is consistent with the hardness of other *Swift* SGRBs, though it is also consistent with the LGRB population. In Figure 2 we plot the hardness and duration of GRB 080503 against other *Swift* bursts, resolving this burst and other short events with extended emission separately into the spike and the extended tail. The properties of the initial spike of GRB 080503 match those of the initial spikes of other SGRBs with extended emission (and are consistent with the population of short bursts lacking extended emission), while the hardness and duration of the extended emission are similar to that of this component in other short bursts.

The fluence of the extended emission measured from 5 s to 140 s after the BAT trigger in the 15–150 keV bandpass is $(1.86 \pm 0.14) \times 10^{-6}$ erg cm^{-2}. The ratio of this value to the spike fluence is very large (∼30 in the 15–150 keV band), higher than that of any previous *Swift* short (or possibly short) event including GRB 060614. It is not, however, outside the range measured for BATSE members of this class, which have measured count ratios up to ∼40 (GRB 931222, Norris & Bonnell 2006). In Figure 4, we plot the fluences in the prompt versus extended emission of all *Swift* SGRBs to date. BATSE bursts are overplotted as solid gray triangles; HETE event GRB 050709 is shown as a star. The two properties appear essentially uncorrelated, and the ratio has a wide dispersion in both directions. Although only two *Swift* events populate the high extended-to-spike ratio portion of the diagram (and the classification of GRB 060614 is controversial), the difference in this ratio between these and more typical events is only about a factor of 10, and the intermediate region is populated by events from BATSE

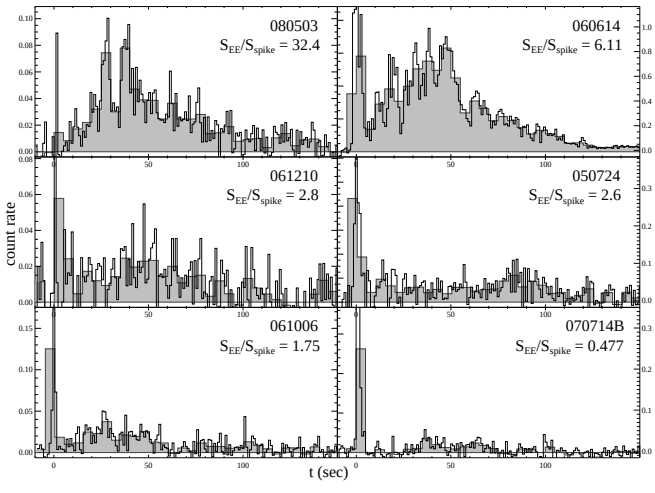

FIG. 3.— BAT 25–100 keV light curves of several different *Swift* short bursts with high signal-to-noise (S/N) extended emission, including GRB 080503 (top left), showing the similar morphology of these events. The 1 s binned curve is plotted as a black line; a 5 s binning is plotted in solid gray to more clearly show the longer-duration extended emission which for most events is near the detection threshold. Possible short GRB 060614 is also shown; it appears very similar to GRB 080503 except that the initial pulse is significantly longer.

and HETE[18], suggesting a continuum in this ratio across what are otherwise similar events.

Lag analysis (Norris et al. 2000) has also been used as a short-long diagnostic. For GRB 080503, the spectral lag between the 50–100 keV and the 25–50 keV bands using the light curves in the 16 ms binning is 1 ± 15 ms (1σ error), consistent with zero and characteristic of short-hard GRBs. Unfortunately, the signal is too weak to measure the spectral lag for the extended emission which dominates the fluence. While lag can vary between pulses in a GRB (Hakkila et al. 2008) and short pulses typically have short lags, even very short pulses in canonical long GRBs have been observed to have non-negligible lags (Norris & Bonnell 2006).

Based on all of these arguments, we associate GRB 080503 with the "short" (Type I) class. Regardless of classification, however, the extremely faint afterglow of this burst appears to be a unique feature. In fact, as we will show, while the extremely low afterglow flux is more reminiscent of SGRBs than LGRBs, relative to the gamma-rays the afterglow is so faint that this event appears quite unlike any other well-studied member of either population to date.

2.2. *UVOT Observations*

The *Swift* UV-Optical Telescope (UVOT) began observations of the field of GRB 080503 at 83 s after the trigger, starting with a finding chart exposure in the White filter at $t = 85$–184 s. No source is detected within the XRT position to a limiting magnitude of >20.0 (Brown & Mao 2008). A sequence of filtered observations followed, and then additional White-band exposures. The transient is not detected in any exposure. Because of the deep Gemini data shortly thereafter, these additional limits do not constrain the behavior of the optical counterpart and are not reported or reanalyzed here.

[18] However, the HETE fluence ratio is in a very different bandpass, and the actual ratio may be significantly lower than the plotted ratio

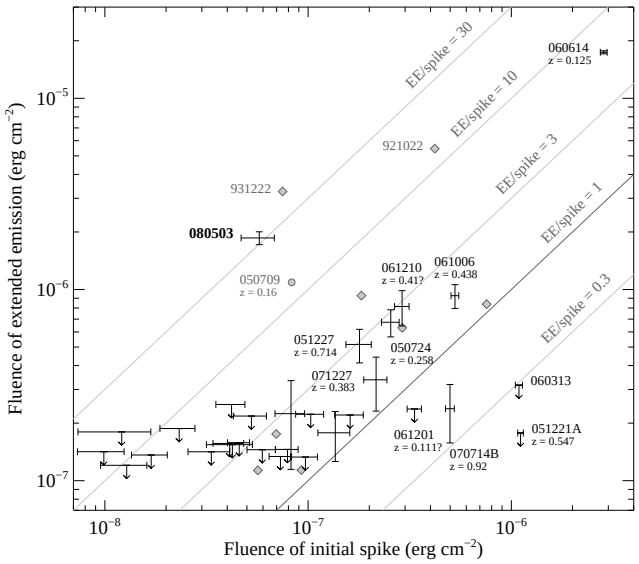

FIG. 4.— Fluences of the short initial spike versus the long extended-emission episode for SGRBs and candidate SGRBs. For *Swift* bursts this is measured in the 15–150 keV band. For BATSE bursts (diamonds) the values are calculated from the count rates in Norris & Bonnell (2006) and fluences (20–100 keV) on the BATSE website. HETE GRB 050709 (circle) is taken from Table 2 of Villasenor et al. (2005) and is in the 2–25 keV band, which is significantly softer than the *Swift* and BATSE bandpasses. In harder bandpasses the extended emission is likely to be much fainter; this point should therefore be treated as an upper limit. BATSE and HETE short bursts without extended emission are not shown. Several properties are worthy of note. First, the extended-to-prompt ratio shows large variance, quite unlike the observed T90 values and hardness ratios. Second, the large majority of *Swift* events without extended emission are very faint bursts — the limits on the extended counterpart are not strongly constraining, although strongly extended emission-dominated events like GRB 080503 do appear to be rare. Third, events with bright extended emission have a wide range of short-spike fluence; the two values are not correlated. Events with known redshift are labeled; no clear trends with distance are evident.

A summary of the the subsequent UVOT observations is given by Brown & Mao (2008).

2.3. *Keck Observations*

Shortly after the GRB trigger we slewed with the 10 m Keck-I telescope (equipped with LRIS) to the GRB position. After a spectroscopic integration on a point source near the XRT position that turned out in later analysis to be a faint star, we acquired (between 13:38:37 and 13:57:02) imaging in the B and R filters simultaneously. Unfortunately, because the instrument had not been focused in imaging mode prior to the target of opportunity, these images are of poorer quality and less constraining than Gemini images (see below) taken at similar times. The optical transient (OT) is not detected in either filter. Magnitudes (calibrated using the Gemini-based calibration, §2.4) are reported in Table 2.

On May 8 we used long-slit ($1''$ wide) spectroscopy with LRIS (Oke et al. 1995) on Keck I to obtain spectra of two relatively bright galaxies $13''$ SE of the afterglow position. We calibrated the two-dimensional spectra with standard arc and internal flat exposures. We employed the 600 line mm^{-1} grism (blue camera) and 600 line mm^{-1} grating blazed at 10,000 Å (red camera).

The data were processed with the LowRedux[19] package within XIDL[20]. Both objects show the same emission lines, at common observed wavelengths of $\lambda_{\rm obs} \approx 5821$, 6778.8, 7592.2, 7745.6, and 7820 Å. The latter two are associated with the Hβ and [O III] λ5007 lines, respectively, identifying this system to be at $z = 0.561$.

While the placement of the slit in the target-of-opportunity spectroscopic on May 3 did not cover the location of the transient, a third, serendipitous object along the slit shows a single emission line at $\lambda_{\rm obs} \approx$ 6802.9 Å and a red continuum. We tentatively identify this feature as unresolved [O II] λ3727 emission and estimate its redshift to be 0.8245. This source is far (31″) from the OT position, at $\alpha = 19^{\rm h}06^{\rm m}31^{\rm s}.1$, $\delta = +68°48'04''.3$.

2.4. *Gemini Observations*

We also initiated a series of imaging exposures using GMOS on the Gemini-North telescope. The first image was a single 180 s r-band exposure, beginning at 13:24, 58 min after the *Swift* trigger. We then cycled through the g, r, i, and z filters with 5×180 s per filter. A second g epoch was subsequently attempted, but the images are shallow due to rapidly rising twilight sky brightness.

The following night (May 4) we requested a second, longer series of images at the same position. Unexpectedly, the transient had actually brightened during the intervening 24 hr, so we continued to observe the source for several additional epochs. The next night (May 5), we acquired r-band images (9×180 s), followed by a long nod-and-shuffle spectroscopic integration, and concluded with 4×180 s exposures in each of the g and i bands. On May 6 and 7, we acquired long r-band imaging only (14×180 s on May 6 and 16×180 s on May 7). Finally, on May 8, we acquired a long K-band integration using NIRI, nearly simultaneous with the *HST* observations (§2.5) at the same epoch.

Optical imaging was reduced using standard techniques via the Gemini IRAF package[21]. Magnitudes were calculated using seeing-matched aperture photometry and calibrated using secondary standards. The standard star field SA 110 was observed on the nights of May 3, May 4, May 5, and May 8; catalog magnitudes (Landolt 1992) were converted to *griz* using the equations from Jester et al. (2005) and used to calibrate 23 stars close to the GRB position (Table 3).

In an attempt to measure or constrain the redshift of GRB 080503, we obtained a nod-and-shuffle long-slit spectroscopic integration of the positions of the optical transient and the nearby faint galaxy S1 (Figure 6). Two exposures of 1320 s each were obtained starting at 12:20 on 2008 May 05. Unfortunately, even after sky subtraction and binning, no clear trace is observed at the position, and no line signatures are apparent. The redshift of the event is therefore unconstrained, except by the g-band photometric detection which imposes a limit of approximately $z < 4$.

[19] http://www.ucolick.org/~xavier/LowRedux/index.html; developed by J. Hennawi, S. Burles, and J. X. Prochaska.

[20] http://www.ucolick.org/~xavier/IDL/index.html .

[21] IRAF is distributed by the National Optical Astronomy Observatory, which is operated by the Association of Universities for Research in Astronomy (AURA) under cooperative agreement with the National Science Foundation.

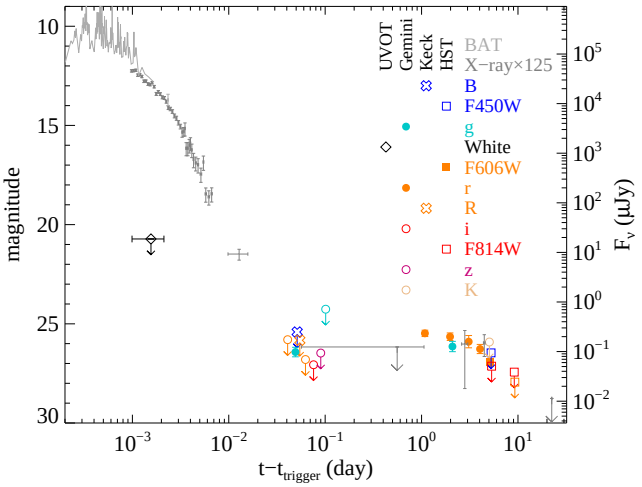

FIG. 5.— X-ray and optical light curves of GRB 080503. The optical bands have been shifted to the r band assuming an optical spectral index of $\beta = 1.2$; the X-ray light curve has been shifted by a factor of 125 to match the optical (corresponding to $\beta_{OX} = 0.75$). The BAT light curve is extrapolated into the X-ray band using the high-energy spectrum. 3σ upper limits are shown with arrows.

We began near-infrared observations of GRB 080503 on 2008 May 08 at 12:46, roughly simultaneous with the *HST* measurement (§2.5). All images were taken in the K_s band with NIRI. We employed the standard Gemini-N dither pattern for each of the 30 s exposures. In all, 92 images were taken yielding a total time on target of ∼1.5 hr. The data were reduced and the individual frames were combined in the usual way using the "gemini" package within IRAF. There is no detection of a source at the location of the optical transient. The nearby faint galaxies (S1 and S4) are also undetected. Calibrating relative to the 2MASS catalog (excluding stars near the edge of the image because NIRI is known to suffer from fringing), we derive an upper limit of $K_s > 22.47$ mag (3σ).

All optical photometry, in conjunction with the space-based measurements from *Swift* and Chandra, is plotted in Figure 5.

2.5. *Hubble Space Telescope Observations*

Given the unusual nature of the afterglow, and the indications of a Li-Paczyński-like light curve in the first two days, we proposed[22] to observe the field of GRB 080503 with the Wide-Field Planetary Camera (WFPC2) on *HST*. Filter changes, depth, and cadences were chosen to confirm or refute the basic predictions of the Li & Paczyński (1998) model (see Fig. 11 and §3.4). The localization region was observed in three epochs on 2008 May 8, May 12, and July 29. A set of F450W (1 orbit), F606W (2 orbits), and F814W (1 orbit) observations were obtained during the first visit, with F606W (2 orbits) and F814W (2 orbits) in the second visit, and finally a deep (4 orbit) observation in F606W in the third visit. Observations were dithered (a 3-point line dither for the first epoch of F450W and F814W, and a standard 4-point box for all other observations). The data were reduced in the standard fashion via `multidrizzle`, while the pixel scale was retained at the native $\sim 0.1''$pixel^{-1}.

At the location of the afterglow in our first-epoch

[22] Program GO-DD 11551; PI Bloom.

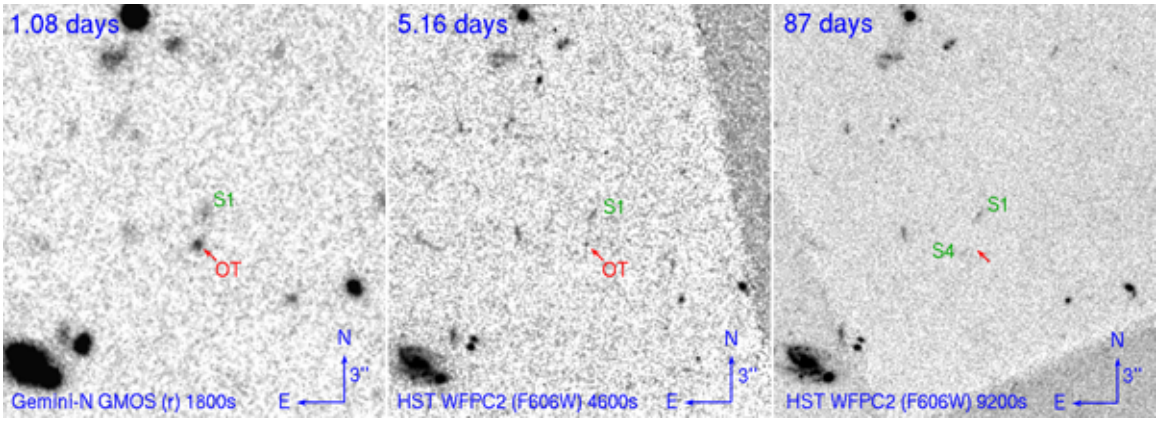

FIG. 6.— Ground-based and space-based images showing the evolution of the faint OT associated with GRB 080503. The transient peaked at about $t = 1$ d, shown in an image from Gemini-North at left. Thereafter it faded rapidly and is barely detected in the first *HST* epoch in F606W only. Later observations failed to reveal a galaxy coincident with the transient position. Two very faint nearby (but non-coincident) galaxies are designated "S1" and "S4."

F606W image we found a faint point source, with a magnitude of F606W $= 27.01 \pm 0.20$ after charge-transfer efficiency correction following Dolphin (2000). Our other observations show no hint of any emission from the afterglow or any host galaxy directly at its position. We derived limits on any object at the GRB position based on the scatter in a large number (~ 100) of blank apertures placed randomly in the region of GRB 080503. The limits for each frame are shown in Table 2. In addition, a stacked frame of all our F814W observations yields F814W > 27.3 mag. A combination of all but our first-epoch F606W observations provides our deepest limit of F606W > 28.5 mag (3σ), in a stacked image with exposure time 13,200 s. Therefore any host galaxy underlying GRB 080503 must be fainter than that reported for any other short burst.

Although there is no galaxy directly at the GRB position, there are faint galaxies close to this position which are plausible hosts. In particular, our stacked image of all the F606W observations shows a faint galaxy $\sim 0.8''$ from the afterglow position, with F606W(AB) $= 27.3 \pm 0.2$ mag (designated "S4" in Figure 6). Although faint, this galaxy is clearly extended, with its stellar field continuing to $\sim 0.3''$ from the GRB position. (It is plausible that deeper observations or images in redder wavebands may extend its disk further, but we have no evidence that this is the case.) Additionally, there is a brighter galaxy ("S1," F606W ≈ 26.3 mag) $\sim 2''$ to the north of the afterglow position, also visible in the Gemini images. Given the faintness of these galaxies and the moderate offset from the afterglow position, the probability of chance alignment is nontrivial (a few percent, following Bloom et al. 2002), and we cannot make firm statements about their association with GRB 080503.

The extremely deep limit on a host galaxy puts GRB 080503 in very rare company. Among short bursts, no comparably deep limit exists for any previous event except GRB 061201, although a study with deep *HST* imaging of short-burst hosts has yet to be published. However, ground-based searches for hosts of other SGRBs with subarcsecond positions have identified coincident host galaxies in 9 of 11 cases. The two exceptions are GRB 061201 (Stratta et al. 2007) and GRB 070809 (Perley et al. 2008); both of these appear at relatively small physical offset from nearby spirals which have been

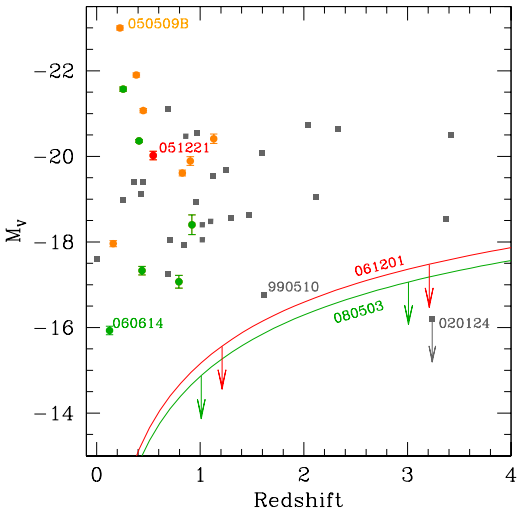

FIG. 7.— The absolute magnitudes and redshifts for a sample of both long (grey squares, from Fruchter et al. 2006) and short GRB hosts. Bursts with extended emission are marked in green and bursts without extended emission are red; orange denotes SGRBs too faint for a strong limit on extended emission fluence to be inferred. The two solid lines represent "host-less" SGRBs 061201 and 080503, and are extrapolated based on the observed limits. Due to the poor wavelength sampling of many faint GRB hosts the absolute magnitudes have been obtained assuming a flat spectrum K-correction $M_V = V - DM + 2.5\log(1+z)$, where DM is the distance modulus. We have assumed a ΛCDM cosmology with $\Omega_M = 0.27$, $\Omega_\Lambda = 0.73$ and $H_0 = 72$ km s^{-1} Mpc^{-1}. The nondetection of a host for GRB 080503 implies either that it lies at higher redshift than the majority of the SGRB population, that it originates from a host which is much fainter than the median, or that it has been ejected to a sufficient distance from its host that it can no longer be firmly associated with it. Such deep limits to hosts underlying GRBs are rare, with only a single LGRB (020124, Berger et al. 2002) undetected in deep HST imaging (out of a sample of ~ 50), while two SGRBs (of roughly 15 with good optical positions) are undetected to similar limits.

claimed as host candidates. Short GRB 070707 has a coincident host with $R = 27.3$ mag (Piranomonte et al. 2008), about the same as the magnitude of the nearest galaxy to the GRB 080503 OT position. In fact, even compared to long bursts, the lack of host galaxy is unusual; only five events have host-galaxy measurements or limits fainter than 28.5 mag.

There are two general possibilities to explain this extreme faintness. First, GRB 080503 could be at high

redshift ($z > 3$), or at moderately high redshift in a very underluminous galaxy (at $z \approx 1$, comparable to the highest-z SGRBs detected to date, $M_B < -15$ mag).[23] A bright "short" GRB at very high redshift would impose a much larger upper end of the luminosity distribution of these events than is currently suspected. An extremely underluminous host would also be surprising under a model associating SGRBs with old stars, since the bulk of the stellar mass at moderate redshifts is still in relatively large galaxies (Faber et al. 2007).

Second, GRB 080503 could be at low redshift but ejected a long distance from its host. To further examine this possibility, we have estimated the probabilities (following Bloom et al. 2002) of a statistically significant association with other bright galaxies in the field. A rather faint spiral galaxy is located 13″ SE of the afterglow position (J2000 coordinates $\alpha = 19^{\rm h}06^{\rm m}31^{\rm s}.7$, $\delta = 68°47'27''.9$; visible in the bottom-left corner of Figure 6) and has $r = 21.7$ mag and $z = 0.561$ (§2.3). The probability that this is a coincidence is of order unity. We also searched NED and DSS image plates for very bright nearby galaxies outside the field. The nearby ($D \approx 5$ Mpc) dwarf galaxy UGC 11411 is located at an offset of 1.5°; again the chance of random association is of order unity. There are no other nearby galaxies of note. While a low probability of random association does not rule out an association with one of these objects (a progenitor that escapes its host-galaxy potential well and has a sufficiently long merger time will be almost impossible to associate with its true host), it prevents us from making an association with any confidence.

2.6. *Swift XRT analysis*

The *Swift* X-ray telescope began observing GRB 080503 starting ∼82 s after the burst, detecting a bright X-ray counterpart. Observations continued during the following hour and in several return visits.

The XRT data were reduced by procedures described by Butler & Kocevski (2007b). The X-ray light curve, scaled to match the optical at late times, is shown in Figure 5. Despite the bright early afterglow, the flux declined precipitously and no significant signal is detected during the second through fourth orbits. A marginally significant detection is, however, achieved during a longer integration a day later.

The X-ray hardness ratio decreases, as does the 0.3–10.0 keV count rate, during the course of the early observations (Figure 8a,b). Absorbed power-law fits to the evolving spectrum are statistically acceptable (χ^2/dof ≈ 1) and yield a photon index Γ which increases smoothly with time and an H-equivalent column density N_H that apparently rises and then falls in time (Figure 8c,d). This unphysical N_H variation is commonly observed in power-law fits to the XRT emission following BAT GRBs and XRT flares (see, e.g., Butler & Kocevski 2007a); it suggests that the intrinsic spectrum, plotted on a log-log scale, has time-dependent curvature. In fact, we find that the combined BAT and XRT data are well fit by a GRB model (Band et al. 1993) with constant high- and low-energy photon indices and a time-decreasing break energy that passes through the XRT band during the observation.

[23] GRB 080503 could also be at moderate redshift $z = 1 - 3$ in a moderately large but extremely dusty galaxy. Even then, our K nondetection imposes strong constraints on the size of the object, and the relatively blue $g - r$ afterglow color suggests that the environment of the GRB is not particularly dust-obscured.

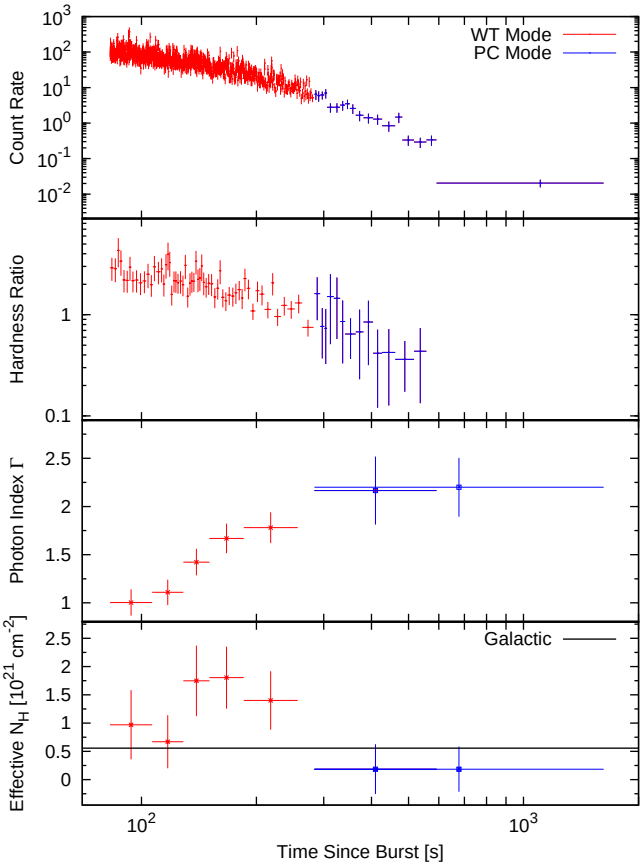

FIG. 8.— (a) The 0.3–10.0 keV X-ray flux measured by the XRT declines rapidly following the bursts. (b) The ratio of counts in the 1.3–10.0 keV to 0.3–1.3 keV bands also declines. (c,d) The spectrum is well modelled by an absorbed power law, although the effective column density N_H appears to unphysically rise and decline during the observations (see text).

The amount of physical column density that contributes to the effective N_H in Figure 8c can be estimated at early or late times, when the effective N_H is near its minimum, or from the Band et al. (1993) GRB model fits. We find $N_H = 5.5^{+1.5}_{-0.9} \times 10^{20}$ cm^{-2}, comparable to the Galactic value of $N_H = 5.6 \times 10^{20}$ cm^{-2}, indicating that the host-galaxy hydrogen column is minimal.

2.7. *Chandra X-Ray Observatory Observations*

Under Director's Discretionary Proposals 09508297 and 09508298, we conducted imaging using the Chandra X-Ray Observatory ACIS-S on two occasions. During the first integration (2008-05-07 19:18:23 to 2008-05-08 04:09:59) an X-ray source is detected at $\alpha = 19^{\rm h}06^{\rm m}28^{\rm s}.76$, $\delta = +68°47'35''.3$ (J2000, 0.5″ uncertainty), consistent with the position of the optical afterglow. This source was not detected during the second epoch (2008-05-25 18:11:36 to 2008-05-26 03:04:28), limiting the decay rate to steeper than approximately $t^{-1.6}$.

Minimizing the Cash (1976) statistic, we find the Chandra spectrum to be acceptably fit by an absorbed power law with $\beta = 0.5 \pm 0.5$ and unabsorbed flux $F_X = (1.5 \pm 0.7) \times 10^{-14}$ ergs cm^{-2} s^{-1} (0.3–10 keV). We assume Galactic absorption only.

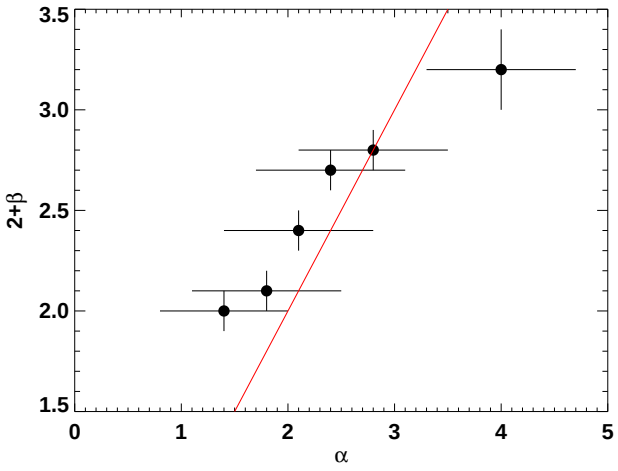

FIG. 9.— Decay index α versus spectral index β (+2) during the rapid-decay phase of the external power-law. For a purely power-law spectrum a closure relation $\alpha = 2 + \beta$ is predicted by the high-latitude (curvature) model; this is approximately obeyed as shown by the solid line. For more complicated spectra this relation may not be obeyed exactly.

We attempted to use the photon arrival times to constrain the temporal index (α) assuming power-law brightening or fading behavior (Butler et al. 2005). The exposure time is short compared to the time elapsed since the GRB, precluding strong constraints. Although the data do marginally favor brightening behavior ($\alpha = -13 \pm 7$), in contrast to the well-established optical fading at this point, we do not consider this to be a strong conclusion.

3. MODELING AND INTERPRETATION

3.1. *The Origin of the Rapid Decay Phase*

Immediately after the prompt emission subsides, the X-ray light curve (Fig. 9) is observed to decline extremely rapidly ($\alpha = 2$–4, where α is defined by $F_\nu \propto t^{-\alpha}$), plummeting from a relatively bright early X-ray flux to below the XRT detection threshold during the first orbit. Although a similar rapid early decline is seen in nearly all GRBs for which early-time X-ray data are available (O'Brien et al. 2006), GRB 080503 probably constitutes the most dramatic example of this on record: the decline of $\sim$6.5 orders of magnitude from the peak BAT flux is larger by a factor of ~ 100 than observed for the reportedly "naked" GRB 050421 (Godet et al. 2006) and comparable to the decline of two other potentially naked *Swift* events described by Vetere et al. (2008). The lack of contamination of this phase of the GRB by any other signature (X-ray flares or a standard afterglow) affords an excellent test for models of this decay component.

An afterglow interpretation can be ruled out almost immediately. In addition to the difficulties faced by such a model in explaining the very sharp decay index, continuous spectral softening, and smooth connection with the prompt emission (all of which are commonly observed in the rapid decay phase of other GRBs), the early UVOT White measurement ($\lesssim$220 μJy at 85–184 s) imposes a limit on the X-ray to optical spectral slope of $\beta_{\rm OX} < -0.5$ (using the convention $F_\nu \propto \nu^{-\beta}$) that is very difficult to explain as afterglow emission, but is consistent with the low-energy tail of prompt-emission spectra.

While the origin of the rapid-decay phase observed in most X-ray light curves is still not settled, the most popular interpretation is high-latitude emission (Kumar & Panaitescu 2000), also referred to as the curvature effect. In this scenario, after the prompt emission ends some photons still reach us from increasingly larger angles relative to the line of sight (to the central source) due to a longer path length induced by the curvature of the (usually assumed to be quasi-spherical) emitting region (or shell). Such late photons correspond to a smaller Doppler factor, resulting in a relation between the temporal and spectral indexes, $\alpha = 2 + \beta$, that holds at late times ($t - t_0 \gg \Delta t$) for each pulse in the prompt light curve (of typical width Δt and onset time t_0) where $\beta = -d\log F_\nu / d\log\nu$ and $\alpha = -d\log F_\nu / d\log(t - t_0)$. The total tail of the prompt emission is the sum of the contributions from the different pulses. At the onset of the rapid-decay phase the flux is usually dominated by the tail of the last spike in the light curve, and therefore can potentially be reasonably fit using a simple single-pulse model with t_0 set to near the onset of this last spike. At later times the tails of earlier pulses can become dominant. At sufficiently late times both $t - t_0 \gg \Delta t$ and $t \gg t_0$ (i.e., $t - t_0 \approx t$) for all pulses, and the relation $\alpha = 2 + \beta$ is reached for $t_0 = 0$ (i.e., setting the reference time t_0 to the GRB trigger time). In GRB 080503 the large dynamic range enables us to probe this late regime; as shown in Figure 9, which displays α versus $2 + \beta$ for the rapid-decay phase using $t_0 = 0$, the relation $\alpha = 2 + \beta$ roughly holds, as expected for high-latitude emission.

While the above discussion suggests that high-latitude emission is a viable mechanism for the rapid-decay phase in GRB 080503, a more careful analysis is called for, especially since assuming an intrinsic power-law spectrum during the rapid-decay phase requires an unphysical time-variable N_H; a better and more physical description is provided by using a fixed Galactic value for $N_{\rm H}$ and an intrinsic Band et al. (1993) spectrum whose peak energy passes through the XRT range (see §2.6). A more detailed analysis of this event (and others) in the context of the high-latitude model and possible alternatives using this model will be forthcoming in future work.

3.2. *Constraining the External Density from Lack of Early Afterglow Emission*

The faintness of the early afterglow is very striking. Any afterglow emission for this event was unlikely to be brighter than about ~ 1 μJy at optical wavelengths and 10^{-2} μJy in X-rays at any time after about 1 hr (and if the late afterglow peak were due to a non-afterglow signature, a possibility we consider in §3.4, these limits would be even more stringent.) Our early optical limits are the deepest for any GRB on record at this epoch (Kann et al. 2008). If the observed emission at $t > 1$ d is due to a mini-SN or other process, the absence of an afterglow is even more notable. Figure 10 shows the X-ray flux at 11 hr, $F_X(11\,{\rm hr})$, and the fluence of the prompt γ-ray emission, S_γ, for GRB 080503 together with a large sample of both LGRBs and SGRBs (data taken from Figure 4 of Nysewander et al. 2008, but modified slightly as described in the caption.) GRB 080503 immediately stands out as a dramatic outlier, with an F_X/S_γ several

orders of magnitude below that of the general population, indicating a poor conversion of the energy left in the flow after the prompt gamma-ray emission into afterglow (emission from the external forward shock). A natural explanation for this difference is a very low external density.

Using the upper limit on the X-ray flux, $F_X(11\,{\rm hr}) < 8.4\times10^{-15}$ erg cm^{-2} s^{-1}, and the measured fluence, $S_\gamma = (1.7\pm0.1)\times10^{-6}$ erg cm^{-2}, we derive constraints on the external density, $n = n_0$ cm^{-3}. Following Granot et al. (2006), it is convenient to use the X-ray afterglow efficiency, $\epsilon_X(t) \equiv tL_X(t)/E_{\rm k,iso}(t)$. We can relate the isotropic equivalent kinetic energy in the afterglow shock, $E_{\rm k,iso}$, to the measured fluence by using the ratio $\eta_{\rm k\gamma} \equiv E_{\rm k,iso}/E_{\gamma,\rm iso}$, which is expected to be of order unity. This gives

$$\epsilon_X = \frac{tF_X(t)}{\eta_{\rm k\gamma}S_\gamma}, \qquad \epsilon_X(t=11\,{\rm hr}) < 8.0\times10^{-5}\eta_{\rm k\gamma}^{-1}\ , \quad (1)$$

where $L_X(t)$ in the definition of ϵ_X is interpreted here as evaluated at $t = 11$ hr and an energy range of 2–10 keV (converted from our reported 0.3–10 keV value assuming $\beta \approx -1$) in the observer frame. This makes it easier to compare this value to the one derived from standard afterglow theory, as is done next.

The value of $\beta_{\rm OX} \approx 0.7$ suggests $p \approx 2.4$ if the cooling break frequency is above the X-rays, $\nu_c > \nu_X$, and a smaller value of p if $\nu_c < \nu_X$. If $\nu_c < \nu_X$ then for $p \approx 2.2$ and $\epsilon_B \ll \epsilon_e$ (using eq. 7 of Granot et al. 2006),

$$\epsilon_X(t=11\,{\rm hr};\nu_c<\nu_X) \approx 10^{-3}\epsilon_{e,-1}^{p-3/2}\epsilon_{B,-2}^{p/4}E_{\rm k,iso,52}^{(p-2)/4} \quad (2)$$

$$\sim 10^{-3}\epsilon_{e,-1}^{0.7}\epsilon_{B,-2}^{0.55}E_{\rm k,iso,52}^{0.05}\ , \quad (3)$$

where $\epsilon_e = 0.1\epsilon_{e,-1}$, $\epsilon_B = 0.01\epsilon_{B,-2}$, and $E_{\rm k,iso} = 10^{52}E_{\rm k,iso,52}$ erg. There is no dependence on the external density as long as $\nu_c < \nu_X$, and the dependence on $E_{\rm k,iso}$ is extremely weak. It does have some dependence on ϵ_e and ϵ_B. However, reproducing the value derived in eq. (1) requires these shock microphysical parameters to assume very low values – not out of the question but on the low end of the values inferred from modeling of the best-monitored GRB afterglows. This is assuming a reasonable efficiency of the gamma-ray emission, $\epsilon_\gamma \lesssim 0.5$, leaving at least a comparable kinetic energy in the outflow that was transferred to the shocked external medium before 11 hr, $\eta_{\rm k\gamma} \approx (1-\epsilon_\gamma)/\epsilon_\gamma \gtrsim 1$. For typical values of the shock microphysical parameters ($\epsilon_e \approx 0.1$ and $\epsilon_B \approx 0.01$), eqs. (1) and (2) can be reconciled either if $\nu_c(11\,{\rm hr}) \gg \nu_X$ (which as is shown below implies a very low external density), or if $1-\epsilon_\gamma \approx \eta_{\rm k\gamma} \ll 1$ (i.e., an extremely high gamma-ray efficiency that leaves very little energy in the afterglow shock, compared to that emitted in gamma-rays).

For a reasonable gamma-ray efficiency ($\epsilon_\gamma \lesssim 0.5$) this suggests that $\nu_c > \nu_X$. In this case the value of ϵ_X is reduced by a factor of $(\nu_c/\nu_X)^{1/2}$ compared to its value for $\nu_c < \nu_X$ (that is given in eq. (2) for $p \approx 2.2$) and is smaller by a factor of $\sim$1.48 for $p \approx 2.4$ (that is inferred from the observed value of $\beta_{\rm OX}$ for $\nu_c > \nu_X$). For a $\nu_X \approx 10^{18}$ Hz (corresponding to ~ 4 keV) this suggests $\nu_c(11\,{\rm hr}) \gtrsim 10^{20}$ Hz, which in turn (using the expression for ν_c from Granot & Sari 2002) implies

$$n \lesssim 5\times10^{-6}E_{\rm k,iso,52}^{-1/2}\epsilon_{e,-1}^{-1}\epsilon_{B,-2}^{-1/2}\ {\rm cm}^{-3}\ . \quad (4)$$

This dependence on the parameters is valid in the limit of $\epsilon_B \ll \epsilon_e$, where $Y \approx (\epsilon_e/\epsilon_B)^{1/2} \gg 1$ and $\nu_c \propto n^{-1}E_{\rm k,iso}^{-1/2}(1+Y)^{-2}\epsilon_B^{-3/2} \propto n^{-1}E_{\rm k,iso}^{-1/2}\epsilon_e^{-1}\epsilon_B^{-1/2}$. Therefore, the upper limit on the external density cannot easily be increased by a large factor. This suggests a very low external density compared to typical disk values ($n \approx 1$ cm^{-3}) or even a Galactic halo ($n \approx 10^{-3}$ cm^{-3}, Basu 2003) but is of the same order as the intergalactic particle density ($n \approx 10^{-6}$ cm^{-3}, Hinshaw et al. 2008). This result therefore provides strong evidence that this explosion occurred far outside any galaxy. (An intriguing alternative to this, however, would be if the burst occurred in a low-density pulsar cavity inflated by one of the NSs in the precursor binary; Rosswog & Ramirez-Ruiz 2003.)

3.3. *Afterglow Models: Why the Delay?*

The counterpart rebrightened during the second night of observations, rising again above detectability in both the optical and X-ray bands. The optical is far better constrained than the X-rays in this case: the rise is at least 1.5 mag (a factor of ~ 3) and peaks between 0.1 and 2 d after the event, though most likely the peak is toward the end of this period as the optical observations at 1–2 d are consistent with constant flux. Although the faint afterglow and sparse observations preclude a careful search for chromatic behavior, the X-ray emission shows a broadly similar temporal behavior as the optical and is consistent with being on the same segment of a power-law spectrum ($F_\nu \propto \nu^{-\beta}$), with a very reasonable value of the optical to X-ray spectral slope for GRB afterglows, $\beta_{\rm OX} \approx 0.7$. This suggests that they arise from the same physical region, and probably also from the same emission mechanism (most likely synchrotron emission from the forward external shock, i.e. the afterglow; we will consider other models in §3.4).

A late peak ($t \approx 1$ d) is unusual for an afterglow but not unprecedented. Most such events are *rebrightenings* and not global maxima. The most prominent examples of this have been long bursts, though some modest X-ray flaring has been observed in a few short GRBs (Fox et al. 2005; Campana et al. 2006), and notably the classification-challenged GRB 060614 had an optical peak between 0.3–0.5 d. Without deep imaging before our first Gemini exposure, we cannot constrain the nature of an optical afterglow in the earliest phases of GRB 080503. However, it is clear that since this behavior is consistent with that observed for at least some previous GRB afterglows, the observed light curve, like the SED, is consistent with an afterglow model. The cause of this delayed peak, however, remains an open question, which we will now turn our attention to.

The similar temporal behavior of the X-ray and optical flux around the observed peak argues against a passage of a spectral break frequency (e.g., the typical synchrotron frequency ν_m passing through the optical) as the source of the late time peak in the light curve, and in favor of a hydrodynamic origin. One possibility for such a hydrodynamic origin is the deceleration time, $t_{\rm dec}$. However, such a late deceleration time implies either an extremely low initial Lorentz factor of the outflow, Γ_0, or an unreasonably low external density

$$n_0 \approx \left[\frac{t_{\rm dec}}{42(1+z)\,{\rm s}}\right]^{-3}E_{\rm k,iso,51}\left(\frac{\Gamma_0}{100}\right)^{-8} \quad (5)$$

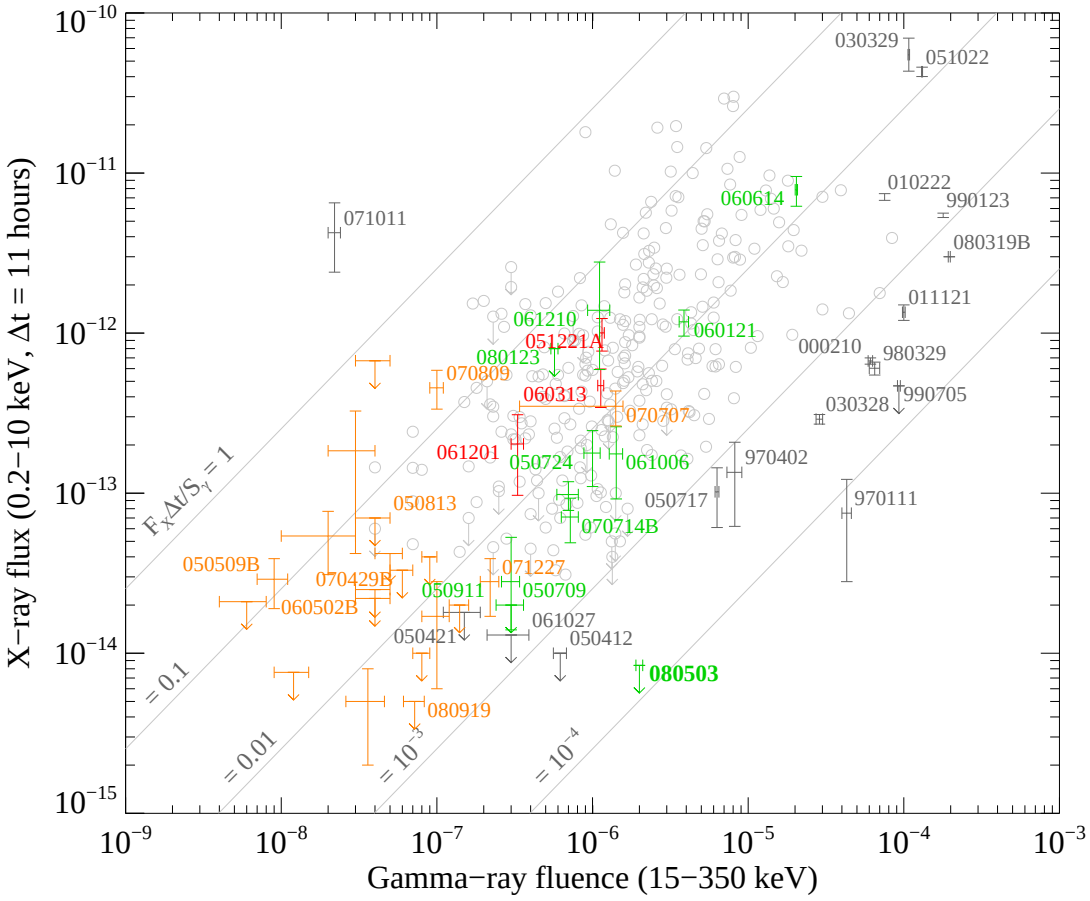

FIG. 10.— Comparison of the total gamma-ray fluence (15–150 keV) versus X-ray flux (0.2–10 keV) at 11 hr post-burst for all GRBs with X-ray afterglows, based on Figure 4 and Tables 1–2 of Nysewander et al. (2008) supplemented with our own re-evaluation of the upper limits on events without detections after ∼10 hr using the *Swift* XRT repository (Evans et al. 2007) and other primary references listed in Nysewander et al. (2008). New SGRBs in 2008 have been added, along with the extremely bright GRB 080319B (Bloom et al. 2008). Long bursts are shown in gray, short bursts without extended emission in red, faint short bursts with poor constraints on extended emission in orange (as in Figure 2), and short bursts with extended emission (including the ambiguous GRB 060614) in green. Prominent events are labeled. Almost all events with detections fall along an approximately linear relation indicating a roughly constant prompt-to-afterglow ratio; most upper limits are not inconsistent with this. GRB 080503 (plotted as an upper limit, though the detection by Chandra at several days after trigger suggests that the flux cannot be much less than this) is strongly discrepant compared to nearly all previous events. GRB 970111 is the first burst for which rapid X-ray observations were conducted and its general faintness appears to be real (Feroci et al. 1998); however, based on the plot in the supplementary material of de Pasquale et al. (2006) the afterglow flux at 11 hr may be somewhat underestimated.

$$\approx 10^{-10} E_{\rm k,iso,51} \left(\frac{\Gamma_0}{100}\right)^{-8} \quad (6)$$

$$\approx E_{\rm k,iso,51} \left(\frac{\Gamma_0}{5.7}\right)^{-8} \quad (7)$$

(see, e.g., Granot 2005; Lee et al. 2005a), where we have used $t_{\rm dec}/(1+z) \approx 1$ d.

An initial Lorentz factor of $\Gamma_0 \gtrsim 100$ is typically required in order to overcome the compactness problem for the prompt GRB emission. This would in turn imply in our case an external density of $n \lesssim 10^{-10}$ cm^{-3} that is unrealistically low, even for the the intergalactic medium (IGM). An external density typical of the IGM, $n_{\rm IGM} \sim 10^{-6}$ cm^{-3} would require $\Gamma_0 \sim 30$. This may or may not be a strong concern in this case: the constraints on the high-energy spectrum of the extended-emission component of short GRBs are not yet well-established[24], and it is not yet certain that existing compactness constraints apply to this emission component, potentially allowing a lower minimum Lorentz factor than is required for SGRB initial spikes (*Fermi* has detected high energy emission up to ∼ 3 GeV from the short GRB 081024B, Omodei 2008) or for classical LGRBs.

An alternative hydrodynamic explanation for the late peak is if the afterglow shock encounters a large and sharp increase in the external density into which it is propagating. However, it would be very hard to produce the required rise in the light curve up to the broad peak due to a sudden jump in the external density (Nakar & Granot 2007) unless a change in the microphysical parameters accompanies the sharp density discontinuity (as may occur inside a pulsar cavity inflated by one of the NSs in the precursor binary.) Below we discuss other possible causes for such a broad and largely

[24] Note, however, that EGRET has detected high-energy emission including a ∼ 1 GeV photon (Sommer et al. 1994) in the extended prompt emission (lasting ∼ 50 s) of the short (< 1 s) GRB 930131 (Kouveliotou et al. 1994).

achromatic peak in the afterglow light curve. The main features these models need to explain are the extremely low value of $F_X(11\,\mathrm{hr})/S_\gamma$ and the late-time peak (a few days) in the afterglow light curve.

Off-axis jet: The bulk of the kinetic energy in the afterglow shock might not be directed along our line of sight, and could instead point somewhat away from us. For such an off-axis viewing angle (relative to the region of bright afterglow emission, envisioned to be a jet of initial half-opening angle θ_0) the afterglow emission is initially strongly beamed away from us (this can be thought of as an extreme version of the "patchy shell" model – Kumar & Piran 2000a; Nakar et al. 2003). As the afterglow jet decelerates the beaming cone of its radiation widens, until it eventually reaches our line of sight, at which point the observed flux peaks and later decays (Rees 1999; Dermer et al. 2000; Granot et al. 2002; Ramirez-Ruiz et al. 2005). This interpretation can naturally account for the dim early afterglow emission (without necessarily implying an extremely low external density), as well as the rapid decay after the peak (if our viewing angle from the jet axis is $\theta_{\rm obs} \gtrsim 2\theta_0$). The possibility of a slightly off-axis jet is particularly intriguing given the fact that the initial spike is much fainter relative to the extended emission in this event (and in GRB 060614, which also exhibits a late light curve peak) than for most SGRBs; one may envision a unified short-burst model in which the short-spike component of the prompt emission is beamed more narrowly than the component associated with the extended emission. However, since a low circumstellar density is no longer needed, there is no natural means of supressing the early afterglow that should be created by the extended-emission associated component, and producing the large ratio of the gamma-ray fluence and early-time X-ray afterglow flux would require that the gamma-ray emission along our line of sight is bright and the gamma-ray efficiency is very large (Eichler & Granot 2006). Regardless of whether the jet is seen off-axis, there is good evidence that this GRB is significantly collimated, with a decay index $\alpha > 2$ at late times ($t > 3$ d) in both the optical and X-ray bands.

Refreshed shock: A "refreshed shock" (Kumar & Piran 2000b; Ramirez-Ruiz et al. 2001; Granot et al. 2003) is a discrete shell of slow ejecta that was produced during the prompt activity of the source and catches up with the afterglow shock at a late time (after it decelerates to a somewhat smaller Lorentz factor than that of the shell), colliding with it from behind and thus increasing its energy. This interpretation also requires a very large gamma-ray efficiency, ($\epsilon_\gamma \gtrsim 95\%$) corresponding to $\epsilon_\gamma/(1-\epsilon_\gamma) \sim \eta_{\rm k\gamma}^{-1} \gtrsim 30$. In this picture, the sharp decay after the peak (at least as steep as $\sim t^{-2}$) requires that the collision occur after the jet-break time.

The rather sparse afterglow data make it hard to distinguish between these options. Nevertheless, the overall observed behavior can be reasonably explained as afterglow emission in the context of existing models for afterglow variability.

3.4. *Constraints on a Mini-Supernova*

Under any scenario, the absence of a bright afterglow associated with GRB 080503, together with the late-time optical rise, suggests that a substantial fraction of this event's energy may be coupled to trans- and non-relativistic ejecta. Non-relativistic outflows from the central engine are sufficiently dense to synthesize heavy isotopes, which may power transient emission via reheating of the (adiabatically cooled) ejecta by radioactive decay (Li & Paczyński 1998). Since at most ~ 0.1 $\mathrm{M}_\odot$ is expected to be ejected from any short GRB progenitor, the outflow becomes optically thin earlier and traps a smaller fraction of the decay energy than for a normal SN; these "mini-SNe" therefore peak earlier and at fainter magnitudes than normal SNe.

Current observational limits (Bloom et al. 2006; Hjorth et al. 2005a; Castro-Tirado et al. 2005; Kann et al. 2008) indicate that any supernova-like event accompanying an SGRB would have to be over 50 times fainter (at peak) than normal Type Ia SNe or Type Ic hypernovae, 5 times fainter than the faintest known SNe Ia or SNe Ic, and fainter than the faintest known SNe II. These limits strongly constrain progenitor models for SGRBs. Unless SGRBs are eventually found to be accompanied by telltale emission features like the SNe associated with LGRBs, the only definitive understanding of the progenitors will come from possible associations with gravitational wave or neutrino signals.

The most promising isotope to produce bright transient emission is ^{56}Ni because its decay timescale of ~ 6 d is comparable to the timescale over which the outflow becomes optically thin. Compact object mergers, however, are neutron rich and are not expected to produce large quantities of Ni (Rosswog et al. 2003). Metzger et al. (2008b) estimate that in the best cases only $\leq 10^{-3}$ $\mathrm{M}_\odot$ of Ni is produced by outflows from the accretion disk. On the other hand, neutron-rich material may be dynamically ejected from a NS–NS or a NS–BH merger. Its subsequent decompression may synthesize radioactive elements through the r process, whose radioactive decay could power an optical transient (Li & Paczyński 1998). Material dynamically stripped from a star is violently ejected by tidal torques through the outer Lagrange point, removing energy and angular momentum and forming a large tail. These tails are typically a few thousand kilometers in size by the end of the disruption event. Some of the fluid (as much as a few hundredths of a solar mass) in these flows is often gravitationally unbound, and could, as originally envisaged by Lattimer & Schramm (1976), undergo r-process nucleosynthesis (Rosswog et al. 1999; Freiburghaus et al. 1999). The rest will eventually return to the vicinity of the compact object, with possible interesting consequences for SGRB late-time emission. A significant fraction ($\sim$ 10–50%) of the accretion disk that initially forms from the merger will also be ejected in powerful winds (Lee et al. 2005b) from the disk at late times; this material is also neutron rich and will produce radioactive isotopes (Metzger et al. 2008c).

In the case of GRB 080503, the amount (mass M) of radioactive material synthesized in the accompanying SGRB wind necessary to provide the observed luminosity is constrained to be $(M/\mathrm{M}_\odot)f \approx (1.5-1.8)\times 10^{-7}\,(z/1)^2$. A larger uncertainty is the value of f, which is the fraction of the rest mass of the radioactive material that is converted to heat and radiated around the optical near the peak of the light curve ($\sim$ 1–2 d). Generally $f \lesssim 10^{-4}$ since $\sim 10^{-3}$ of the rest mass is converted to gamma-rays

during the radioactive decay, only part of the gamma-ray energy is converted to heat (some gamma-rays escape before depositing most of their energy), and only part of mass in the synthesized radioactive elements decays near the peak of the light curve (so that f can easily be much less than 10^{-4}, but it is hard for it to be higher than this value). We note here that the most efficient conversion of nuclear energy to the observable luminosity is provided by the elements with a decay timescale comparable to the timescale it takes the ejected debris to become optically thin (t_τ). In reality, there is likely to be a large number of nuclides with a very broad range of decay timescales. Current observational limits thus place interesting constraints on the abundances and the lifetimes of the radioactive nuclides that form in the rapid decompression of nuclear-density matter — they should be either very short or very long when compared to t_τ so that radioactivity is inefficient in generating a high luminosity.

In Figure 11 we show two light-curve models for a Ni-powered mini-SN from GRB 080503 calculated according to the model of Kulkarni (2005) and Metzger et al. (2008b). Shown with asterisks and triangles are the r-band and F606W band detections and upper limits from Gemini and *HST*. The solid and dashed lines correspond to a low-redshift ($z = 0.03$) and high-redshift ($z = 0.5$) model, respectively. Qualitatively, both models appear to be reasonably consistent with the flux light curve. To reproduce the peak of the optical emission at $t \approx 1$ d, a total ejected mass of ~ 0.1 M$_\odot$ is required in either model. In order to reproduce the peak flux, the Ni mass required in the high- and low-redshift models is $M_{\rm Ni} \approx 0.3$ M$_\odot$ and 2×10^{-3} M$_\odot$, respectively. Since the former is unphysically large in any SGRB progenitor model, a high-redshift event appears inconsistent with a mini-SN origin for the optical rise.

If GRB 080503 originates at very low redshift ($z < 0.1$), a mini-SN model would still appear viable. However, most mini-SN models also predict that the spectrum should redden significantly with time and possess a negative spectral slope once the outflow becomes optically thin after the peak at $t \approx 1$ d; the *HST* detection in F606W and non-detections in F814W and F450W at 5.35 d, however, suggest that the spectrum is approximately flat at late times. While the detected optical emission may be attributed to a mini-SN type of event, the expected spectrum in such a case is quasi-thermal, resulting in no detectable emission in the X-rays. (Rossi & Begelman 2008 have proposed a fallback model in which X-rays can rebrighten days or weeks after the event, but the luminosity is extremely low, and to explain the Chandra count rate a very close distance of ~ 8 Mpc would be required; while not excluded by our data, this is orders of magnitude closer than any known non-magnetar short gamma-ray burst.) Therefore, the late X-ray detections a few days after the GRB are most likely afterglow emission.

4. CONCLUSIONS

The very same faintness which makes GRB 080503 so remarkable unfortunately also makes it difficult to strongly constrain various physical interpretations of this event. However, the combination of the extremely low limit on the afterglow-to-prompt fluence ratio shortly after the burst and the lack of a coincident host galaxy provides strong evidence that this burst exploded in a very low-density (possibly even intergalactic) medium.

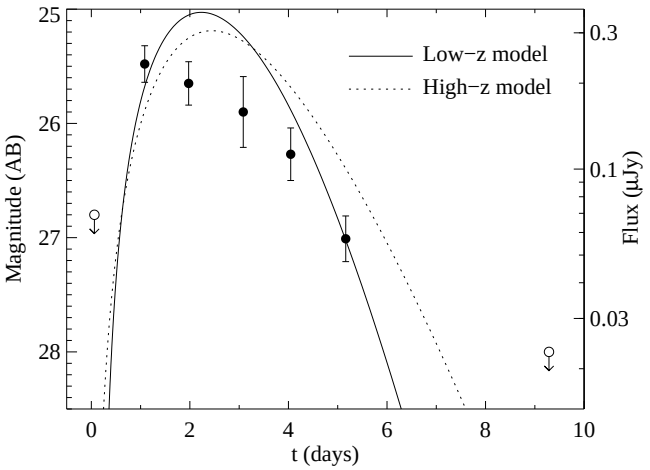

FIG. 11.— Two AB magnitude (Oke 1974) light-curve models for a Ni-powered "mini-SN" from GRB 080503, based on the model of Li & Paczyński (1998), Kulkarni (2005), and Metzger et al. (2008b). The solid line indicates a model at $z = 0.03$ with a ^{56}Ni mass $\approx 2 \times 10^{-3}$ M$_\odot$, total ejecta mass ≈ 0.4 M$_\odot$, and outflow velocity $\approx 0.1c$. The dotted line is for a pure Ni explosion at $z = 0.5$ with mass ≈ 0.3 M$_\odot$ and velocity $\approx 0.2c$. Also shown are our r-band and F606W detections and upper limits from Gemini and *HST*.

This result has several important implications for the nature of "short" bursts and of GRB classification in general. For example, the interpretation of GRB 060614 (and whether it groups more naturally with canonical "short" events like GRB 050724, canonical "long" events like 080319B, or in a new class entirely on its own) is clarified somewhat. GRB 060614, despite having a prompt-extended light-curve morphology (as well as negligible lag and no supernova to deep limits) was (like GRB 080503) strongly dominated by extended emission but also had a very long spike T_{90} (5.5 s), on the extreme end of the short class. The initial pulse of GRB 080503 was unambiguously short; furthermore, the faint afterglow and lack of host galaxy both provide evidence that this event occurred in an environment quite unlike those of canonical "long" GRBs. The existence of an apparent continuity between the appearance of the light curves of GRB 060614 and GRB 080503 and more traditional short bursts (in stark contrast to the bewildering diversity in the structure of longer GRBs) suggests that they originate from the same or similar progenitors, in spite of the apparent diversity in environments and redshifts. The presence of bright extended emission in GRB 080503, and the prompt-like behavior of its fading tail in the X-ray band, is a counterexample to the inference that extended emission is an environment- or progenitor-correlated phenomenon (Troja et al. 2008). We note again that in the vast majority of cases observed by *Swift*, we cannot strongly constrain the presence of extended emission, and in only two events are limits sufficiently deep to constrain the extended-to-spike fluence ratio to less than the value observed for GRB 070714B.

This same result, however, may pose difficulties to the most popular model of short GRBs: NS–NS or NS–BH merger events. The possibility that the luminosity of the extended emission can exceed that of the ini-

tial spike by factors of 30 or more is problematic for a merger, in which the majority of the accretion disk is expected to accrete within a viscous timescale — not more than a few seconds (Rosswog 2007; Lee et al. 2004). This may strengthen the case for alternative models, such as accretion-induced collapse (Vietri & Stella 1999; Katz & Canel 1996; MacFadyen et al. 2005). On the other hand, the extremely low circumburst density is much more consistent with a merger event with its possibility of a natal kick than models such as accretion-induced collapse. One possible means of avoiding this difficulty in a merger scenario (but which could also apply to other models) would be if, for GRB 080503 and GRB 060614, the prompt spike were focused in a narrow jet seen nearly off-axis while the extended emission were more widely beamed. Such a scenario could occur in the case of compact object mergers if the relativistic jet is collimated by a neutrino-heated baryon wind from the accretion disk at early times (Levinson & Eichler 2000; Rosswog et al. 2003), but the collimating effect of the wind become less effective at later times as the neutrino flux and wind luminosity decreases.

The observed late peak in the optical light curve, which we suspected initially may have been the signature of a Li-Paczyński supernova, is explained reasonably by other models. The peak time of $\sim$1 d is too long to be explained by the deceleration timescale, even for a burst exploding into the extremely low-density intergalactic medium, unless the Lorentz factor associated with the extended episode is also very low. However, an off-axis jet, or alternatively a slower shell of ejecta that catches up with the initially very weak afterglow shock and energizes it (a "refreshed shock"), could produce a rebrightening and a late peak. A rather similar late peak has been observed before in several long bursts and in GRB 060614. Some contribution to the afterglow from a mini-SN is not ruled out but is not necessary to explain the available data.

Our failure to conclusively detect a mini-SN signature may also have significant observational implications. In spite of the "nakedness" of this event vastly suppressing the late-time afterglow flux, any possible mini-SN that may have been associated with this event was concealed by the late-time afterglow. Similar events in a higher-density environment (such as a galactic disk) will have even brighter afterglows. If mini-SN phenomena exist in nature, our observations suggest it will be extremely difficult to detect them over the glow of the relativistic shock created by the burst itself. Our best opportunity is likely to lie in observationally and intrinsically faint events like GRB 050509B, whose weak gamma-ray signal results from a low-energy flow insufficient to create a bright afterglow even in a relatively dense medium, but is bright enough for localization.

J.S.B.'s group is supported in part by the Hellman Faculty Fund, Las Cumbres Observatory Global Telescope Network, and NASA/*Swift* Guest Investigator grant NNG05GF55G. BM and EQ were supported in part by the David and Lucile Packard Foundation, NASA grant NNG05GO22H, and the NSF-DOE Grant PHY-0812811. J.G. gratefully acknowledges a Royal Society Wolfson Research Merit Award. N.R.B. is partially supported by US Department of Energy SciDAC grant DE-FC02-06ER41453 and by a NASA GLAST/Fermi Fellowship. A.V.F. is partially supported by NSF grant AST–0607485 and the TABASGO Foundation. This work was supported in part by NASA (Swift NX07AE98G, ER-R) and DOE SciDAC (DE-FC02-01ER41176, ER-R).

This research is based in part on observations obtained at the Gemini Observatory, which is operated by the Association of Universities for Research in Astronomy, Inc., under a cooperative agreement with the NSF on behalf of the Gemini partnership. Some of the data presented herein were obtained at the W. M. Keck Observatory, which is operated as a scientific partnership among the California Institute of Technology, the University of California, and the National Aeronautics and Space Administration (NASA). The Observatory was made possible by the generous financial support of the W. M. Keck Foundation.

We thank the *HST* and Chandra X-ray Observatory directors and scheduling teams for their extremely rapid turnaround time for observations of GRB 080503. We also thank the Gemini observing staff, in particular T. Geballe, for excellent support, and D. A. Kann for helpful commentary on the manuscript.

REFERENCES

Abbott, B., et al. 2004, Nucl. Instrum. Methods, A517
—. 2008, ApJ, 681, 1419
Acernese, F. et al. 2004, Astroparticle Physics, 21, 1
Band, D., et al. 1993, ApJ, 413, 281
Basu, B. 2003, An Introduction to Astrophysics (Published by PHI Learning Pvt. Ltd.)
Berger, E., et al., Sheppard, S. S., & Songaila, A. 2007, ApJ, 664, 1000
—. 2002, ApJ, 581, 981
—. 2005, Nature, 438, 988
Bloom, J. S., Sigurdsson, S., & Pols, O. R. 1999, MNRAS, 305, 763
Bloom, J. S., Kulkarni, S. R., & Djorgovski, S. G. 2002, AJ, 123, 1111
Bloom, J. S., et al. 2006, ApJ, 638, 354
—. 2007, ApJ, 654, 878
Bloom, J. S., Butler, N. R., & Perley, D. A. 2008, in American Institute of Physics Conference Series, Vol. 1000, American Institute of Physics Conference Series, ed. M. Galassi, D. Palmer, & E. Fenimore, 11–15
Brown, P. J., & Mao, J. 2008, GCN Circular 7675
Burrows, D. N., et al. 2005, Space Science Reviews, 120, 165
Butler, N. R., & Kocevski, D. 2007a, ApJ, 663, 407
—. 2007b, ApJ, 668, 400
Butler, N. R., et al. 2005, ApJ, 621, 884
Campana, S., et al. 2006, A&A, 454, 113
Cash, W. 1976, A&A, 52, 307
Castro-Tirado, A. J., et al. 2005, A&A, 439, L15
Cenko, S. B., et al. 2008, ArXiv e-prints, 0802.0874
Cohen, M., Wheaton, W. A., & Megeath, S. T. 2003, AJ, 126, 1090
Covino, S., et al. 2006, A&A, 447, L5
de Pasquale, M., et al. 2006, A&A, 455, 813
Dermer, C. D., Chiang, J., & Mitman, K. E. 2000, ApJ, 537, 785
Dolphin, A. E. 2000, PASP, 112, 1397
Eichler, D., & Granot, J. 2006, ApJ, 641, L5
Eichler, D., et al. 1989, Nature, 340, 126
Evans, P. A., et al. 2007, A&A, 469, 379
Faber, S. M., et al. 2007, ApJ, 665, 265
Feroci, M., et al. 1998, A&A, 332, L29
Fox, D. B., et al. 2005, Nature, 437, 845
Freiburghaus, C., Rosswog, S., & Thielemann, F.-K. 1999, ApJ, 525, L121
Fruchter, A. S., et al. 2006, Nature, 441, 463

Fryer, C. L., Woosley, S. E., & Hartmann, D. H. 1999, ApJ, 526, 152
Fynbo, J. P. U., et al. 2006, Nature, 444, 1047
Gal-Yam, A., et al. 2006, Nature, 444, 1053
Gehrels, N., et al. 2004, ApJ, 611, 1005
—. 2006, Nature, 444, 1044
—. 2005, Nature, 437, 851
Godet, O., et al. 2006, A&A, 452, 819
Gorosabel, J., et al. 2006, A&A, 450, 87
Granot, J. 2005, ApJ, 631, 1022
Granot, J., Königl, A., & Piran, T. 2006, MNRAS, 370, 1946
Granot, J., Nakar, E., & Piran, T. 2003, Nature, 426, 138
Granot, J., Panaitescu, A., Kumar, P., & Woosley, S. E. 2002, ApJ, 570, L61
Granot, J., & Sari, R. 2002, ApJ, 568, 820
Hakkila, J., et al. 2008, in American Institute of Physics Conference Series, Vol. 1000, American Institute of Physics Conference Series, ed. M. Galassi, D. Palmer, & E. Fenimore, 109–112
Hinshaw, G., et al. 2009, ApJS, 180, 225
Hjorth, J., et al. 2005a, ApJ, 630, L117
—. 2005b, Nature, 437, 859
Janka, H.-T., Eberl, T., Ruffert, M., & Fryer, C. L. 1999, ApJ, 527, L39
Jester, S., et al. 2005, AJ, 130, 873
Kann, D. A., et al. 2008, ArXiv e-prints, 0804.1959
Katz, J. I., & Canel, L. M. 1996, ApJ, 471, 915
Kluzniak, W., & Lee, W. H. 1998, ApJ, 494, L53+
Kouveliotou, C., et al. 1993, ApJ, 413, L101
—., et al. 1994, ApJ, 422, L59
Kulkarni, S. R. 2005, ArXiv e-prints, astroph/0510256
Kumar, P., & Panaitescu, A. 2000, ApJ, 541, L51
Kumar, P., & Piran, T. 2000a, ApJ, 535, 152
—. 2000b, ApJ, 532, 286
Landolt, A. U. 1992, AJ, 104, 340
Lattimer, J. M., & Schramm, D. N. 1976, ApJ, 210, 549
Lee, W. H., & Ramirez-Ruiz, E. 2007, New Journal of Physics, 9, 17
Lee, W. H., Ramirez-Ruiz, E., & Granot, J. 2005a, ApJ, 630, L165
Lee, W. H., Ramirez-Ruiz, E., & Page, D. 2004, ApJ, 608, L5
—. 2005b, ApJ, 632, 421
Levan, A. J., et al. 2006, ApJ, 648, L9
Levinson, A., & Eichler, D. 2000, Physical Review Letters, 85, 236
Li, L.-X., & Paczyński, B. 1998, ApJ, 507, L59
MacFadyen, A. I., Ramirez-Ruiz, E., & Zhang, W. 2005, ArXiv e-prints, astroph/0510192
Mazets, E. P., et al. 1981, Ap&SS, 80, 3
Meszaros, P., & Rees, M. J. 1992, ApJ, 397, 570
Metzger, B. D., Quataert, E., & Thompson, T. A. 2008a, MNRAS, 385, 1455
Metzger, B. D., Piro, A. L., & Quataert, E. 2008b, MNRAS, 390, 781
—. 2008c, ArXiv e-prints 0810.2535
Mochkovitch, R., Hernanz, M., Isern, J., & Martin, X. 1993, Nature, 361, 236
Nakar, E. 2007, Phys. Rep., 442, 166
Nakar, E., & Granot, J. 2007, MNRAS, 380, 1744
Nakar, E., Piran, T., & Granot, J. 2003, New Astronomy, 8, 495
Narayan, R., Paczynski, B., & Piran, T. 1992, ApJ, 395, L83
Norris, J. P., & Bonnell, J. T. 2006, ApJ, 643, 266
Norris, J. P., Cline, T. L., Desai, U. D., & Teegarden, B. J. 1984, Nature, 308, 434
Norris, J. P., Marani, G. F., & Bonnell, J. T. 2000, ApJ, 534, 248
Nysewander, M., Fruchter, A. S., & Pe'er, A. 2008, ArXiv e-prints 0806.3607
O'Brien, P. T., et al. 2006, ApJ, 647, 1213
Ohno, M., et al. 2008, PASJ, 60, 361
Oke, J. B. 1974, ApJS, 27, 21
Oke, J. B., et al. 1995, PASP, 107, 375
Omodei, N. 2008, GCN Circular 8407
Paczynski, B. 1991, Acta Astronomica, 41, 257
Perley, D. A., Foley, R. J., Bloom, J. S., & Butler, N. R. 2006, GCN Circular 5387
Perley, D. A., et al. 2008, GCN Circular 7889
Piranomonte, S., et al. 2008, A&A, 491, 183
Prochaska, J. X., et al. 2006, ApJ, 642, 989
Ramirez-Ruiz, E., et al. 2005, ApJ, 625, L91
Ramirez-Ruiz, E., Merloni, A., & Rees, M. J. 2001, MNRAS, 324, 1147
Rees, M. J. 1999, A&AS, 138, 491
Rossi, E. M., & Begelman, M. C. 2008, ArXiv 0808.1284
Rosswog, S. 2007, MNRAS, 376, L48
Rosswog, S., Liebendörfer, M., Thielemann, F.-K., Davies, M. B., Benz, W., & Piran, T. 1999, A&A, 341, 499
Rosswog, S., & Ramirez-Ruiz, E. 2003, MNRAS, 343, L36
Rosswog, S., Ramirez-Ruiz, E., & Davies, M. B. 2003, MNRAS, 345, 1077
Sakamoto, T., et al. 2006, ArXiv e-prints astro-ph/0605717
Schlegel, D. J., Finkbeiner, D. P., & Davis, M. 1998, ApJ, 500, 525
Soderberg, A. M., et al. 2005, ApJ, 627, 877
Sommer, M., et al. 1994, ApJ, 422, L63
Stratta, G., et al. 2007, A&A, 474, 827
Thöne, C. C., et al. 2008, ApJ, 676, 1151
Troja, E., King, A. R., O'Brien, P. T., Lyons, N., & Cusumano, G. 2008, MNRAS, 385, L10
Vetere, L., et al. 2008, in American Institute of Physics Conference Series, Vol. 1000, American Institute of Physics Conference Series, ed. M. Galassi, D. Palmer, & E. Fenimore, 191–195
Vietri, M., & Stella, L. 1999, ApJ, 527, L43
Villasenor, J. S., et al. 2005, Nature, 437, 855
Woosley, S. E., & Bloom, J. S. 2006, ARA&A, 44, 507
Zhang, B., et al. 2007, ApJ, 655, L25

TABLE 1
PROMPT EMISSION PROPERTIES OF SWIFT SGRBS AND CANDIDATE SGRBS

GRB	ambiguous?	z	$S_{\rm EE}/S_{\rm spike}$
050509B	N	0.2249	< 14.3
050724	N	0.258	2.64 ± 0.49
050813	N	0.722?	< 3.64
050906	Y[a]	-	< 14.87
050911	Y[b c]	0.1646?	1.31 ± 0.43
050925	Y[d]	-	< 1.83
051105A	N	-	< 8.06
051210	Y[b]	0.114?	2.72 ± 1.33
051221A	Y[b]	0.5465	< 0.16
051227	Y[b]	-	2.87 ± 0.677
060313	N	-	< 0.29
060502B	N	0.287?	< 3.45
060801	N	1.131?	< 1.84
060614	Y[b e]	0.125	6.11 ± 0.25
061006	Y[b]	0.4377	1.75 ± 0.26
061201	N	0.111?	< 0.71
061210	N	0.41?	2.81 ± 0.63
061217	N	0.827	< 3.81
070209	N	-	< 8.08
070429B	N	0.904	< 2.44
070714B	N	0.92	0.477 ± 0.163
070724A	N	0.457	< 4.24
070729	N	-	< 2.16
070731	Y[b]	-	< 1.37
070809	Y[b]	0.219?	< 1.37
070810B	N	-	< 9.40
070923	N	-	< 5.96
071112B	N	-	< 4.14
071227	Y[b]	0.383	1.56 ± 0.49[f]
080503	Y[e]	-	32.41 ± 5.7

[a] SGR flare in IC 328?
[b] Spike $T_{90} > 1$ s.
[c] Extended-emission episode is of much shorter duration than in all other events.
[d] Soft event; in Galactic plane.
[e] Fluence dominated by extended emission.
[f] Significance of the extended emission is $< 4\sigma$.

TABLE 2
Optical and Near-IR Observations of the Optical Counterpart of GRB 080503

$t_{\rm mid}$ (day)	Exp. time (s)	filter	magnitude	λ (Å)	flux (or limit) (μJy)	telescope
0.00156	98	white	> 20	3850	< 14.2	Swift UVOT
0.04083	180	r	> 25.80	6290	< 0.204	Gemini-N GMOS
0.04916	800	g	26.76 ± 0.24	4858	0.0890 ± 0.0176	Gemini-N GMOS
0.06250	800	r	> 26.80	6290	< 0.0811	Gemini-N GMOS
0.05125	300	B	> 26.00	4458	< 0.209	Keck I LRIS
0.05458	630	R	> 25.60	6588	< 0.208	Keck I LRIS
0.07583	800	i	> 26.80	7706	< 0.0779	Gemini-N GMOS
0.09000	800	z	> 26.00	9222	< 0.161	Gemini-N GMOS
0.10125	360	g	> 24.60	4858	< 0.650	Gemini-N GMOS
1.08333	1800	r	25.48 ± 0.16	6290	0.273 ± 0.037	Gemini-N GMOS
1.97500	1620	r	25.65 ± 0.19	6290	0.234 ± 0.038	Gemini-N GMOS
2.09167	720	g	26.48 ± 0.26	4858	0.115 ± 0.024	Gemini-N GMOS
3.08333	2700	r	25.90 ± 0.31	6290	0.186 ± 0.046	Gemini-N GMOS
4.04583	2880	r	26.27 ± 0.23	6290	0.132 ± 0.025	Gemini-N GMOS
5.20833	2760	K_s	> 22.47	21590	< 0.700	Gemini-N NIRI
5.35833	4600	F606W	27.01 ± 0.20	6000	0.067 ± 0.011	HST WFPC2
5.35833	2100	F450W	> 26.9	4500	< 0.080	HST WFPC2
5.35833	2100	F814W	> 26.8	8140	< 0.077	HST WFPC2
9.12917	4000	F814W	> 27.1	6000	< 0.058	HST WFPC2
9.12917	4000	F606W	> 28.0	6000	< 0.027	HST WFPC2

Note. — SDSS magnitudes are given in AB, while B and R are under the Vega system. K_s is relative to the 2MASS system (Cohen et al. 2003). Flux values given are corrected for foreground extinction ($E_{B-V} = 0.06$, Schlegel et al. 1998) while magnitudes are uncorrected. Limits are 3σ values.

TABLE 3
Magnitudes of Faint Secondary Standards in the GRB 080503 Field

RA (hh:mm:ss)	dec (dd:mm:ss)	g (mag)	r (mag)	i (mag)	z (mag)	B (mag)	V (mag)	R (mag)	I (mag)
19:06:16.785	+68:46:41.39	19.890	18.677	18.116	17.611	20.496	19.185	18.363	17.562
19:06:27.931	+68:46:55.62	21.338	20.790	20.671	20.410	21.736	21.017	20.602	20.217
19:06:40.791	+68:47:14.20	20.894	20.412	20.324	20.103	21.272	20.612	20.235	19.881
19:06:47.096	+68:47:44.06	20.394	19.308	19.008	18.622	20.961	19.762	19.044	18.508
19:06:25.306	+68:48:47.91	18.552	17.882	17.776	17.457	18.988	18.161	17.685	17.313
19:06:31.664	+68:48:32.11	19.158	17.851	17.349	16.847	19.794	18.398	17.537	16.803
19:06:25.808	+68:47:18.09	21.583	20.428	20.040	19.625	22.171	20.911	20.145	19.524
19:06:33.303	+68:48:01.76	22.115	20.725	19.555	18.840	22.777	21.307	20.305	18.887
19:06:42.332	+68:48:05.17	18.885	18.453	18.412	18.187	19.247	18.632	18.287	17.974
19:06:26.337	+68:46:57.77	23.241	21.868	21.077	20.510	23.898	22.443	21.506	20.483
19:06:42.896	+68:48:08.70	21.778	21.238	21.066	20.696	22.174	21.462	21.043	20.585
19:06:38.937	+68:47:44.69	19.863	19.421	19.361	19.129	20.228	19.604	19.251	18.920
19:06:29.508	+68:47:49.97	23.138	21.832	20.560	19.793	23.774	22.379	21.405	19.870
19:06:39.266	+68:47:48.01	19.900	19.085	18.872	18.542	20.382	19.425	18.859	18.394
19:06:34.192	+68:46:35.61	19.806	19.179	19.040	18.756	20.229	19.440	18.981	18.579
19:06:33.173	+68:46:33.32	20.870	20.333	20.208	19.946	21.265	20.556	20.145	19.753
19:06:29.230	+68:46:10.00	22.166	20.792	19.444	18.661	22.823	21.368	20.348	18.741
19:06:29.556	+68:46:12.79	23.156	22.015	21.577	21.144	23.740	22.492	21.726	21.052
19:06:18.146	+68:47:56.94	23.169	21.896	21.373	20.906	23.794	22.429	21.582	20.831
19:06:29.343	+68:46:23.23	24.127	22.729	21.678	21.039	24.791	23.315	22.326	21.039
19:06:37.946	+68:48:28.37	24.313	23.088	21.740	20.917	24.923	23.601	22.657	21.030
19:06:30.838	+68:48:06.34	24.127	22.581	21.503	20.803	24.838	23.229	22.161	20.849
19:06:21.135	+68:48:18.82	24.853	23.538	22.316	21.578	25.491	24.089	23.118	21.637

Note. — Magnitudes of calibration stars in the field of GRB 080503 as measured using repeated observations of the SA 110 field at varying airmasses over four photometric nights. Uncertainties in all cases are dominated by color terms and are approximately 0.02–0.05 mag.